Elevation of cellular Mg^{2+} levels by the Mg^{2+} transporter, Alr1, supports growth of polyamine-deficient *Saccharomyces cerevisiae* cells

Received for publication, June 6, 2019, and in revised form, September 17, 2019 Published, Papers in Press, September 22, 2019, DOI 10.1074/jbc.RA119.009705

Ashleigh S. Hanner[‡], Matthew Dunworth[§], Robert A. Casero, Jr.[§], Colin W. MacDiarmid[¶], and Myung Hee Park[‡1]

From the [‡]Molecular and Cellular Biochemistry Section, NIDCR, National Institutes of Health, Bethesda, Maryland 20892, [§]Department of Oncology, Sidney Kimmel Comprehensive Cancer Center at The Johns Hopkins University, Baltimore, Maryland 21287, and [¶]Department of Nutritional Sciences, University of Wisconsin, Madison, Wisconsin 53706

Edited by Ronald C. Wek

The polyamines putrescine, spermidine, and spermine are required for normal eukaryotic cellular functions. However, the minimum requirement for polyamines varies widely, ranging from very high concentrations (mM) in mammalian cells to extremely low in the yeast *Saccharomyces cerevisiae*. Yeast strains deficient in polyamine biosynthesis (*spe1*Δ, lacking ornithine decarboxylase, and *spe2*Δ, lacking SAM decarboxylase) require externally supplied polyamines, but supplementation with as little as 10^{-8} M spermidine restores their growth. Here, we report that culturing a *spe1*Δ mutant or a *spe2*Δ mutant in a standard polyamine-free minimal medium (SDC) leads to marked increases in cellular Mg^{2+} content. To determine which yeast Mg^{2+} transporter mediated this increase, we generated mutant strains with a deletion of *SPE1* or *SPE2* combined with a deletion of one of the three Mg^{2+} transporter genes, *ALR1*, *ALR2*, and *MNR2*, known to maintain cytosolic Mg^{2+} concentration. Neither Alr2 nor Mnr2 was required for increased Mg^{2+} accumulation, as all four double mutants (*spe1*Δ *alr2*Δ, *spe2*Δ *alr2*Δ, *spe1*Δ *mnr2*Δ, and *spe2*Δ *mnr2*Δ) exhibited significant Mg^{2+} accumulation upon polyamine depletion. In contrast, a *spe2*Δ *alr1*Δ double mutant cultured in SDC exhibited little increase in Mg^{2+} content and displayed severe growth defects compared with single mutants *alr1*Δ and *spe2*Δ under polyamine-deficient conditions. These findings indicate that Alr1 is required for the up-regulation of the Mg^{2+} content in polyamine-depleted cells and suggest that elevated Mg^{2+} can support growth of polyamine-deficient *S. cerevisiae* mutants. Up-regulation of cellular polyamine content in a Mg^{2+}-deficient *alr1*Δ mutant provided further evidence for a cross-talk between Mg^{2+} and polyamine metabolism.

The polyamines putrescine ($NH_2(CH_2)_4NH_2$), spermidine ($NH_2(CH_2)_3NH(CH_2)_4NH_2$), and spermine ($NH_2(CH_2)_3NH(CH_2)_4NH(CH_2)_3$) are ubiquitous in living cells and organisms and are normally present at high concentrations (mM) (1–3). In the yeast *Saccharomyces cerevisiae*, putrescine is produced from ornithine by ornithine decarboxylase (Spe1; Scheme 1*A*). Spermidine is produced from putrescine, and spermine is produced from spermidine by addition of an aminopropyl moiety from decarboxylated SAM, which is produced by SAM decarboxylase (Spe2; Scheme 1*A*). As the primary and secondary amino groups of polyamines are protonated at physiological pH, polyamines interact with negatively charged molecules such as nucleic acids, proteins, and phospholipids and influence their conformation, stability, and activity (4). The polyamines regulate a large number of cellular processes, including the enhancement of the efficiency and fidelity of translation (5). They are vital for survival of eukaryotes and are intimately involved in the regulation of eukaryotic cell growth. However, the precise modes of their action in supporting many cellular functions are not fully understood.

A high level (mM) of cellular polyamines is required for mammalian cell proliferation, and polyamine homeostasis is tightly regulated by intricate mechanisms (6). Numerous studies have demonstrated the antiproliferative effects of various inhibitors of polyamine biosynthesis or polyamine analogs that cause depletion of polyamines in mammals. The high polyamine requirement of mammalian cells is the rational basis of targeting the polyamine pathways in cancer chemoprevention and chemotherapies (1). Depletion of spermidine and spermine mediated by overexpression of the polyamine catabolic enzyme spermidine/spermine N^1-acetyltransferase 1 also caused a dramatic inhibition of protein synthesis and cell growth (7). In contrast to mammalian cells, the polyamine requirement is extremely low in the yeast *S. cerevisiae*. A *spe2*Δ mutant strain, which is unable to synthesize spermidine and spermine, grew at a nearly normal rate in medium containing 10^{-8} M spermidine, a condition in which the cellular spermidine content dropped as low as 0.2% of WT levels (8).

One clearly defined function of the polyamine spermidine in eukaryotes is its role as precursor of the unusual amino acid hypusine (N^{ϵ}-4-amino-2-hydroxybutyl(lysine)) (9), which is formed by the post-translational modification of the eukaryotic translation factor eIF5A. The aminobutyl moiety of spermidine is conjugated to a specific lysine residue to form deoxyhypusine, which is subsequently hydroxylated to hypusine. Hypusine/de-

This work was supported by the intramural program of the National Institute of Dental and Craniofacial Research, National Institutes of Health (M. H. P.), NIH R01-CA204345 (R. A. C.), and by NIH R01-GM56285 (C. W. M.). The authors declare that they have no conflicts of interest with the contents of this article. The content is solely the responsibility of the authors and does not necessarily represent the official views of the National Institutes of Health.

[1] To whom correspondence should be addressed: Molecular and Cellular Biochemistry Section, Bldg. 30, Rm. 3A300, NIDCR, National Institutes of Health, 30 Convent Dr., Bethesda, MD 20892–4340. Tel.: 301-496-5056; E-mail: mhpark@nih.gov.

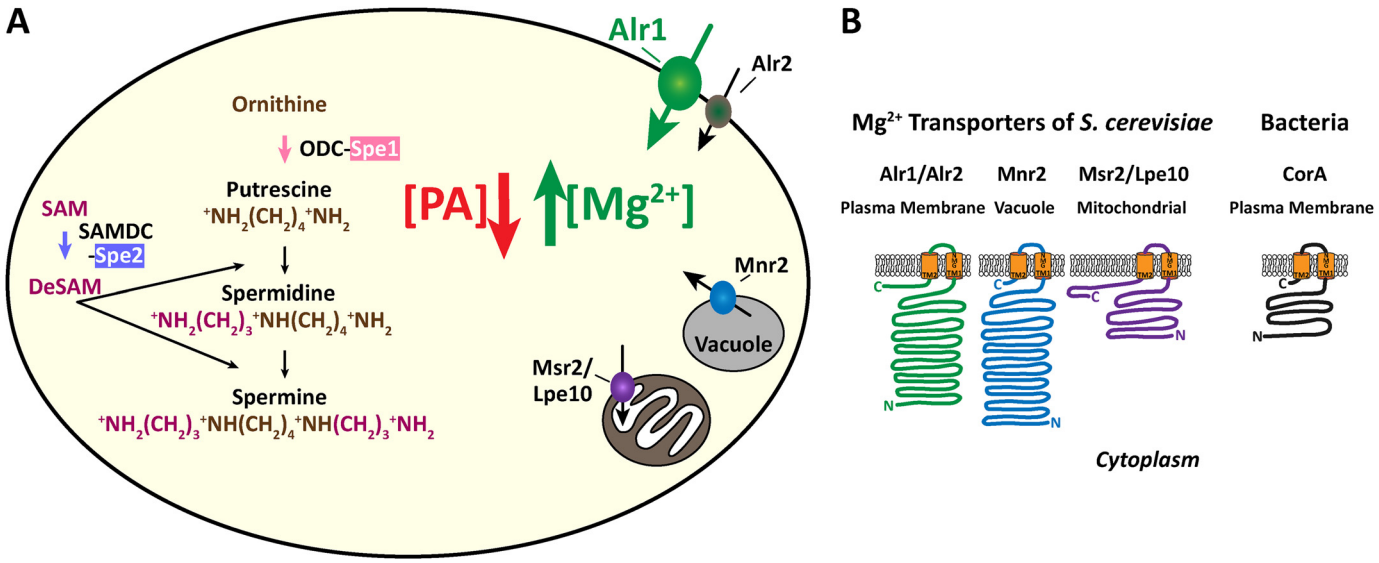

Scheme 1. The polyamine pathway and the Mg^{2+} transporters in *S. cerevisiae* and the inverse relation between cellular polyamines and Mg^{2+}. *A*, the polyamine biosynthesis pathway is shown on the *left side*. Deletion of *SPE1* causes loss of all three polyamines, and deletion of *SPE2* causes depletion of spermidine and spermine with increased accumulation of putrescine. Five *S. cerevisiae* Mg^{2+} transporters are depicted on the *right side*. Of these, Alr1 is mainly responsible for the elevation of Mg^{2+} content upon depletion of polyamines in *S. cerevisiae*. *B*, diagrammatic representation of five *S. cerevisiae* Mg^{2+} transporters in relation to the bacterial Mg^{2+} transporter CorA. Of these, Alr1, Alr2, and Mnr2 are important in the maintenance of cytoplasmic Mg^{2+} concentration. Each Mg^{2+} transporter contains two transmembrane domains near the C terminus that are connected by a short periplasmic loop. Each *turn* in the peptide chain represents 50 amino acids. The conserved GMN signature sequence critical for selective recognition of Mg^{2+} is indicated. *PA*, polyamines; *ODC*, ornithine decarboxylase; *SAMDC*, SAM decarboxylase; *DeSAM*, decarboxylated SAM.

oxyhypusine is essential for the activity of eIF5A. Eukaryotic cell proliferation and animal development depend on hypusinated eIF5A (10, 11). Normally, <2% of cellular spermidine is used for hypusine synthesis in eukaryotic cells. However, in a yeast *spe2*Δ mutant cultured in a medium containing $<10^{-8}$ M spermidine, spermidine became severely limiting, and as much as ~50% of the total cellular spermidine was mobilized for hypusine synthesis. These findings suggest that hypusination of eIF5A is the most critical function of polyamines in yeast, and that, unlike mammalian cells, yeast do not require a high intracellular concentration of polyamines for growth.

The apparent discrepancy in the minimal polyamine requirement between yeast and mammalian cells may be due to differences in the intrinsic functional roles of polyamines, or it may indicate that yeast possess a unique mechanism to compensate for polyamine deficiency. One such mechanism could be the compensatory accumulation of another cation such as magnesium (Mg^{2+}), the most abundant divalent cation in cells (12, 13). Mg^{2+} is a critical cofactor for over 300 enzymes, and it also serves a structural role by stabilizing protein domains. Like polyamines, the majority of cellular Mg^{2+} is bound to negatively charged ligands such as ATP, RNA, DNA, or phospholipids (12). Functional overlap between polyamines and Mg^{2+} has been suggested by several *in vitro* studies. Polyamines stimulated translation in cell-free lysates when Mg^{2+} concentration was suboptimal (4, 14), suggesting that polyamines and Mg^{2+} can partially substitute for each other in protein synthesis. However, there is little information on the *in vivo* functional interaction between polyamines and Mg^{2+} in the regulation of eukaryotic cell growth.

The cellular content of Mg^{2+} is tightly controlled in yeast cells and remains constant over a range of 1–100 mM external Mg^{2+} (15, 16). However, when cells are cultured in low Mg^{2+} medium (<100 μM), intracellular Mg^{2+} content is substantially reduced, and growth is limited (15). Regulation of cellular Mg^{2+} is likely achieved by control of uptake systems, efflux from the cell, and sequestration within organelles (12, 13, 15) (Scheme 1*A*).

To mediate this regulation, yeast express five known Mg^{2+} transporters, all related to the bacterial plasma membrane Mg^{2+} transporter CorA (Scheme 1*B*): Alr1/Alr2 of plasma membrane, Mnr2 of the vacuolar membrane, and Mrs2/Lpe10 of the mitochondrial membrane (15, 17). The CorA superfamily of Mg^{2+} transporters share certain structural features, including two adjacent transmembrane domains near the C terminus that are connected by a short loop (Scheme 1*B*), although the amino acid sequences of the CorA/Mrs2/Alr1 superfamily have diverged significantly, and Alr1/Alr2 and Mnr2 have long N-domains compared with CorA and Mrs2/Lpe10. The universally conserved signature motif, GMN, near the end of the first transmembrane domain is important for the selectivity of Mg^{2+} uptake (18, 19). Alr1 was first identified as a factor whose overexpression confers resistance to aluminum, an inhibitor of CorA proteins (20). Loss of Alr1 function reduced cellular Mg^{2+} content, and mutants lacking Alr1 displayed a severe growth defect. Alr2 is closely related to Alr1 in sequence but contributes little to Mg^{2+} homeostasis and cell growth except in the absence of Alr1 (15, 20–22). Mnr2 is a vacuolar membrane protein required for release of Mg^{2+} from storage vacuoles to the cytoplasm (15). Mrs2 and Lpe10 are two related mitochondrial membrane proteins required for the entry of Mg^{2+} into the mitochondrial matrix (23). Both are required for mitochondrial function but do not influence whole-cell Mg^{2+} accumulation nor do they contribute to the intracellular storage of excess Mg^{2+} (15).

To investigate the relationship between polyamines and Mg^{2+} in yeast cells, we first examined the effect of the *spe1*Δ

Table 1
List of S. cerevisiae strains used in this study

Strains	Genotype	Ref.
Y534/BY4741 (WT)	*MATa, his3Δ1, leu2Δ0, met15Δ0, ura3Δ0*	Chattopadhyay *et al.* (8) and Giaever and Nislow (25)
Y535 (*spe1*Δ)	*MATa, his3Δ1, leu2Δ0, met15Δ0, ura3Δ0, spe1Δ::KAN^R*	Chattopadhyay *et al.* (8) and Giaever and Nislow (25)
Y536 (*spe1*Δ)	*MATa, his3Δ1, leu2Δ0, met15Δ0, ura3Δ0, spe2Δ::KAN^R*	Chattopadhyay *et al.* (8) and Giaever and Nislow (25)
DY1457 (WT)	*MATa, ade6, can1–100$_{oc}$, his3–11,15, leu2–3,112, trp1–1, ura3–52*	Lim *et al.* (29)
AH1 (*spe1*Δ)	*MATa, ade6, can1–100$_{oc}$, his3–11,15, leu2–3,112, trp1–1, ura3–52, spe1Δ::KAN^R*	This study
AH2 (*spe2*Δ)	*MATa, ade6, can1–100$_{oc}$, his3–11,15, leu2–3,112, trp1–1, ura3–52, spe2Δ::KAN^R*	This study
CM200/NP10 (*alr1*Δ)	*MATa, ade6, can1–100$_{oc}$, his3–11,15, leu2–3,112, trp1–1, ura3–52, alr1::HIS3*	Pisat *et al.* (15)
AH3 (*alr1*Δ, *spe2*Δ)	*MATa, ade6, can1–100$_{oc}$, his3–11,15, leu2–3,112, trp1–1, ura3–52, alr1::HIS3, spe2Δ::KAN^R*	This study
NP27 (*alr2*Δ)	*MATa, can1–100$_{oc}$, his3–11,15, leu2–3,112, trp1–1, ura3–52, alr2::TRP1*	Pisat *et al.* (15)
AH4 (*alr2*Δ, *spe1*Δ)	*MATa, can1–100$_{oc}$, his3–11,15, leu2–3,112, trp1–1, ura3–52, alr2::TRP1, spe1Δ::KAN^R*	This study
AH5 (*alr2*Δ, *spe2*Δ)	*MATa, can1–100$_{oc}$, his3–11,15, leu2–3,112, trp1–1, ura3–52, alr2::TRP1, spe2Δ::KAN^R*	This study
NP174 (WT)	*MATa, ade2, can1–100$_{oc}$, his3–11,15, leu2–3,112, trp1–1, ura3–52*	Pisat *et al.* (15)
AH6 (*spe1*Δ)	*MATa, ade2, can1–100$_{oc}$, his3–11,15, leu2–3,112, trp1–1, ura3–52, spe1Δ::KAN^R*	This study
AH7 (*spe2*Δ)	*MATa, ade2, can1–100$_{oc}$, his3–11,15, leu2–3,112, trp1–1, ura3–52, spe2Δ::KAN^R*	This study
NP180 (*mnr2*Δ)	*MATa, ade2, can1–100$_{oc}$, his3–11,15, leu2–3,112, trp1–1, ura3–52, mnr2::SpHIS5*	Pisat *et al.* (15)
AH8 (*mnr2*Δ, *spe1*Δ)	*MATa, ade2, can1–100$_{oc}$, his3–11,15, leu2–3,112, trp1–1, ura3–52, mnr2::SpHIS5, spe1Δ::KAN^R*	This study
AH9 (*mnr2*Δ, *spe2*Δ)	*MATa, ade2, can1–100$_{oc}$, his3–11,15, leu2–3,112, trp1–1, ura3–52, mnr2::SpHIS5, spe2Δ::KAN^R*	This study

mutation (which blocks synthesis of all polyamines) or the *spe2*Δ mutation (which blocks synthesis of spermine and spermidine) on cellular Mg^{2+} content. Interestingly, cellular Mg^{2+} content increased in response to polyamine depletion. Examination of double mutant strains lacking one polyamine biosynthesis gene (*SPE1* or *SPE2*) and one Mg^{2+} transporter gene (*ALR1*, *ALR2*, or *MNR2*) indicated that Alr1 alone was required for this elevated Mg^{2+} accumulation. Consistent with this observation, Alr1 was found to be essential for the survival and growth of polyamine-deficient *spe1*Δ and *spe2*Δ cells. These findings provide strong evidence that yeast can specifically compensate for polyamine deficiency by up-regulating the accumulation of Mg^{2+} ions. The elevation of the cellular polyamine levels in the Mg^{2+}-deficient *alr1*Δ mutant cultured in YPD[2] further suggests an interaction between polyamine and Mg^{2+} metabolism.

Results

Depletion of cellular polyamines leads to an elevation of Mg^{2+} content in S. cerevisiae

We compared the growth, polyamine content, and Mg^{2+} content of WT yeast (Y534; BY4741) and the two polyamine biosynthesis mutants Y535 (*spe1*Δ) and Y536 (*spe2*Δ) (Table 1 and Fig. 1). In Fig. 1 (and Figs. 3 and 4), all data are color-coded (parental strains (*brown*), *spe1*Δ mutant (*pink*), and *spe2*Δ mutant (*blue*)). For comparison of growth, cells were initially inoculated at a very low density (0.0003), and the optical density was followed for 72 h. Cultures were regularly diluted into fresh medium to maintain log phase. In YPD rich in polyamines, the mutations had no effect on growth (Fig. 1*A*), as the mutants utilized polyamines supplied from the medium. Growing cultures for long periods in polyamine-free SDC led to the depletion of initial polyamine stores in *spe1*Δ and *spe2*Δ mutants. The growth of Y535 (*spe1*Δ) and Y536 (*spe2*Δ) in SDC declined with time and stalled after 20–40 h (Fig. 1*B*), and the growth defects were magnified with prolonged incubation. The content of spermidine and spermine in the mutants grown in YPD was only slightly less than that in the WT (Fig. 1*C*). A higher level of putrescine was observed in *spe2*Δ, resulting from the blockage of conversion of putrescine to spermidine and spermidine to spermine in the absence of SAM decarboxylase (Spe2) (Scheme 1*A*). The *spe1*Δ cells cultured in SDC did not contain any detectable polyamines, and *spe2*Δ cells contained a highly elevated level of putrescine but no spermidine or spermine (Fig. 1*D*) as expected. The Y536 (*spe2*Δ) strain grew better than Y535 (*spe1*Δ) in SDC, suggesting that the high level of putrescine partially fulfilled the polyamine requirement.

To determine the effect of these changes in polyamine content on Mg^{2+} homeostasis, parallel samples of Y534 (WT), Y535 (*spe1*Δ), and Y536 (*spe2*Δ) cells were also taken for analysis of their elemental content. There was little or no difference in Mg^{2+} content among the three strains after growth in YPD (3.1–3.3 mg of Mg^{2+}/g dry weight) (Fig. 1*E*). However, after 24-h culture in SDC, the Mg^{2+} content of the polyamine-deficient *spe1*Δ and *spe2*Δ cells increased substantially (by ~2.5- and ~1.6-fold, respectively) (Fig. 1*F*). The increase was consistently more pronounced in *spe1*Δ than *spe2*Δ cells, suggesting that the degree of Mg^{2+} accumulation was responsive to the severity of polyamine deficiency. To verify that this change in Mg^{2+} content was a consequence of polyamine deficiency and not the absence of some other component of YPD in SDC, Mg^{2+} content was also measured in cells cultured in SDC supplemented with 10^{-8} or 10^{-6} M spermidine (Fig. 1, *G* and *H*). The elevation in cellular Mg^{2+} content of the mutants was reduced by spermidine supplementation. When cultured in SDC containing 10^{-8} M spermidine, Mg^{2+} content increased ~2.1-fold in *spe1*Δ and ~1.4-fold in *spe2*Δ (Fig. 1*G*). We chose this concentration of spermidine, as the *spe2*Δ mutants can grow nearly normally in SDC containing 10^{-8} M spermidine when cellular polyamines were limiting (0.2% of normal level) (8). A strong increase in the Mg^{2+} content under this condition

[2] The abbreviations used are: YPD, yeast extract–peptone–dextrose medium; SDC, synthetic dextrose complete medium; SD, synthetic dextrose medium; dansyl, 5-dimethylaminonaphthalene-1-sulfonyl; ANOVA, analysis of variance; ICP-OES, inductively coupled plasma optical emission spectrometry.

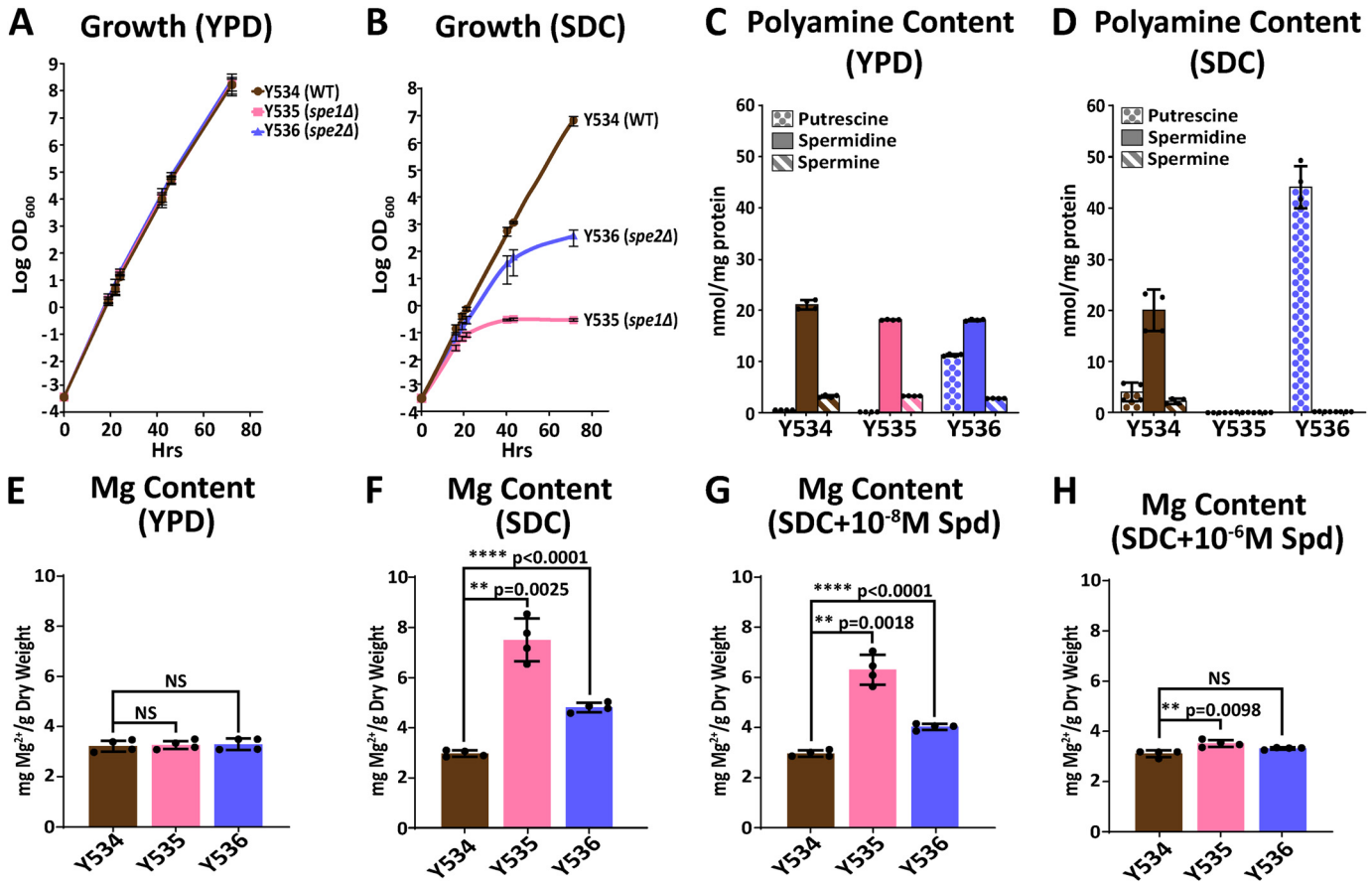

Figure 1. Analysis of growth and polyamine and Mg^{2+} content of Y534 (WT), Y535 (*spe1*Δ), and Y536 (*spe2*Δ) strains. *A* and *B*, growth of yeast strains (Y534, Y535, and Y536) at 30 °C in YPD (*A*) and SDC (*B*) was analyzed over 72 h. The cells were inoculated at a starting density of 0.0003 OD_{600} and diluted down to 0.001 when the density reached an OD_{600} of ~1. Data *points* indicate means and *error bars* represent S.E. ($n = 4$). *C* and *D*, cells were inoculated in YPD (*C*) and SDC (*D*) at 0.001, and ~10–20 OD_{600} units of cells were harvested at a density of ~1 OD_{600} for analyses of polyamines. The content of putrescine, spermidine, and spermine is displayed separately for each strain. *E*, *F*, *G*, and *H*, Mg^{2+} content of three strains cultured in YPD (*E*), SDC (*F*), SDC + 10^{-8} M spermidine (*Spd*) (*G*), and SDC + 10^{-6} M spermidine (*H*) and harvested as above is shown. The values of polyamine and Mg^{2+} content are indicated as *black dots*, and each *bar* indicates the mean and the *error bars* represent S.D. ($n = 4$). The *p* values were calculated by ANOVA. *p* values less than 0.05 were considered statistically significant: **, $p \leq 0.01$; ****, $p \leq 0.0001$ compared with the control. *NS* indicates that the difference is not significant.

suggests that Mg^{2+} elevation contributes to the nearly normal growth of the mutant. When cells were supplemented with a much higher level of spermidine (10^{-6} M), only small increases in Mg^{2+} content were observed (13.2 and 6.8% in *spe1*Δ and *spe2*Δ, respectively) (Fig. 1*H*), confirming an inverse relationship between spermidine supply and Mg^{2+} accumulation by the mutant strains.

To determine whether this effect of polyamine deficiency was specific to Mg^{2+} or reflected a more general effect on nutrient accumulation, we examined the content of potassium (K), manganese (Mn), zinc (Zn), and phosphorus (P) (Table 2). Only small variations (<13%) in potassium content were observed in the three strains cultured in YPD, SDC, and SDC supplemented with spermidine. No consistent negative or positive effect of polyamine depletion was observed on the content of potassium, indicating that polyamine deficiency does not cause accumulation of cations in general. Like the Mg^{2+} content, the Zn^{2+} content of Y535 and Y536 cells was increased after culture in SDC (~3- and ~1.4-fold, respectively), and the elevated Zn content was reduced in cells cultured in SDC supplemented with spermidine. In contrast, the Mn^{2+} content was not elevated in response to polyamine depletion. These results suggest that Mg^{2+} and Zn^{2+} are transported by the same transporter, Alr1, but Mn^{2+} is not. A moderate increase in phosphorus content was observed in *spe1*Δ cells when polyamines were depleted and cellular Mg^{2+} was substantially increased. This effect is consistent with previous reports showing a close relationship between Mg^{2+} content and phosphate accumulation by yeast (15, 24). Overall, these data indicate that a major effect of polyamine depletion is elevation of the Mg^{2+} content, perhaps mediated by a change in transporter activity.

Generation of mutant strains with a combined deletion of a polyamine biosynthesis gene and a Mg^{2+} transporter gene

As yeast responded to polyamine deficiency by increasing Mg^{2+} accumulation, we suspected that this increase was essential to maintaining viability and growth. If so, inactivation of one of the required Mg^{2+} transporters might prevent Mg^{2+} accumulation and compromise the growth of polyamine-deficient cells. To examine this possibility, we constructed a set of double mutant strains combining the *spe1*Δ or *spe2*Δ mutation with a mutation in one of the three Mg^{2+} transporters (Alr1, Alr2, or Mnr2) (Scheme 1, *A* and *B*), known to be important in the regulation of cytosolic Mg^{2+} concentration (15). Double

Table 2

Contents of K, Mg, Mn, P, and Zn in Y534, Y535, and Y536 strains cultured in different medium

The contents of Mg and other elements were determined by ICP-OES using 10–20 OD_{600} units of Y534, Y535, and Y536 cells cultured in four different media. The values (mg/g dry weight) are means ± S.D. ($n \geq 4$). Spd, spermidine.

Medium	Strain	K	Mg	Mn	P	Zn
		mg/g dry weight	*mg/g dry weight*	*mg/g dry weight*	*mg/g dry weight*	*mg/g dry weight*
YPD	Y534 (WT)	23.39 ± 2.37	3.16 ± 0.22	0.0042 ± 0.0006	26.81 ± 1.95	0.3878 ± 0.0526
YPD	Y535 (*spe1*Δ)	20.70 ± 0.74	3.23 ± 0.16	0.0043 ± 0.0004	26.26 ± 2.28	0.4194 ± 0.0677
YPD	Y536 (*spe2*Δ)	22.27 ± 0.96	3.25 ± 0.23	0.0042 ± 0.0004	27.00 ± 2.32	0.4114 ± 0.0664
SDC	Y534 (WT)	19.82 ± 1.87	3.00 ± 0.13	0.0062 ± 0.0012	22.14 ± 0.37	0.2014 ± 0.0222
SDC	Y535 (*spe1*Δ)	20.18 ± 3.13	7.53 ± 0.85	0.0029 ± 0.0016	27.66 ± 0.63	0.6058 ± 0.0571
SDC	Y536 (*spe2*Δ)	21.07 ± 2.11	4.84 ± 0.19	0.0034 ± 0.0012	26.48 ± 1.62	0.2757 ± 0.0384
SDC + Spd (10^{-8} M)	Y534 (WT)	20.99 ± 1.07	3.00 ± 0.13	0.0066 ± 0.0005	23.38 ± 0.62	0.1816 ± 0.0436
SDC + Spd (10^{-8} M)	Y535 (*spe1*Δ)	21.84 ± 2.98	6.34 ± 0.60	0.0060 ± 0.0012	26.10 ± 4.89	0.2741 ± 0.0102
SDC + Spd (10^{-8} M)	Y536 (*spe2*Δ)	19.06 ± 0.32	4.07 ± 0.12	0.0067 ± 0.0008	23.88 ± 0.46	0.1403 ± 0.0345
SDC + Spd (10^{-6} M)	Y534 (WT)	20.79 ± 1.00	3.11 ± 0.13	0.0068 ± 0.0007	22.95 ± 2.16	0.1852 ± 0.0411
SDC + Spd (10^{-6} M)	Y535 (*spe1*Δ)	21.16 ± 1.32	3.52 ± 0.14	0.0068 ± 0.0009	22.30 ± 0.69	0.1978 ± 0.0377
SDC + Spd (10^{-6} M)	Y536 (*spe2*Δ)	20.26 ± 0.73	3.32 ± 0.04	0.0064 ± 0.0007	23.31 ± 1.57	0.1598 ± 0.0082

mutant strains were constructed by deletion of *SPE1* or *SPE2* in the Mg^{2+} transport mutant strains CM200 (*alr1*Δ), NP27 (*alr2*Δ), and NP180 (*mnr2*Δ) by transformation with a PCR-amplified *spe1*Δ*::KanMX4* or *spe2*Δ*::KanMX4* marker (25) and selection of G418-resistant clones. Transformation of two isogenic parental strains (DY1457 for CM200 and NP27, and NP174 for NP180) was also performed in parallel. New *spe1*Δ and *spe2*Δ strains representing all combinations of mutations were isolated successfully (AH1–AH9; Table 1) with the exception of the *spe1*Δ *alr1*Δ strain. The inability to isolate this mutant suggests that the combination of the two mutations was lethal. The knockout status of the five genes, *SPE1*, *SPE2*, *ALR1*, *ALR2*, and *MNR2*, in the parental strains and the nine new knockout mutants (AH1–AH9) was confirmed by PCR (Fig. 2) using an ORF primer set and a knockout primer set (Table 3). For each *spe1*Δ and *spe2*Δ mutant, a PCR product with an expected size was detected with a knockout primer set but not with an ORF primer set.

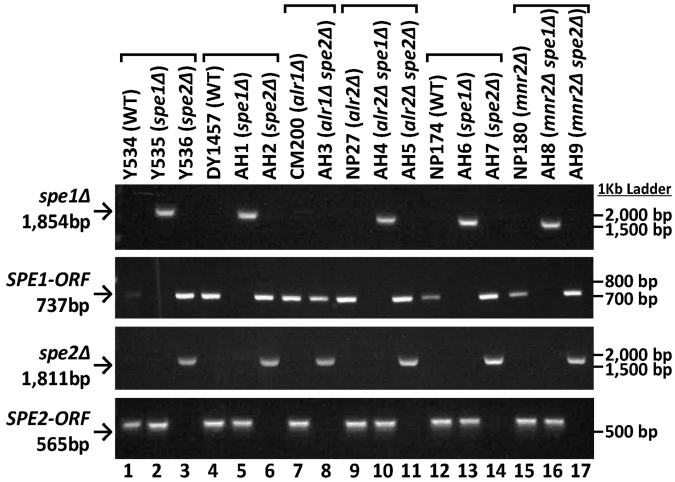

Figure 2. Validation of parental strains and *spe1*Δ and *spe2*Δ mutant strains by PCR. The status of *SPE1* and *SPE2* genes was determined in six sets of isogenic strains marked by *bars* above the strain names. Knockout of the *SPE1* or *SPE2* gene was confirmed by the presence of a PCR product with a knockout primer set and the absence of a PCR product using an ORF primer set. From each of the four sets of PCR reactions (four panels), one main product (either a knockout PCR product or an ORF PCR product) was generated, consistent with each genotype. The positions of 1-kb ladder DNA standards flanking the PCR product are marked on the *right side* of each panel.

Efficient Mg^{2+} uptake by Alr1 is essential for survival and growth of polyamine-deficient cells

To determine the effect of lack of a Mg^{2+} transporter in polyamine deficiency, we first compared the growth of each of the *spe1*Δ and *spe2*Δ mutants derived from the WT DY1457 and the two mutants, CM200 (*alr1*Δ) and NP27 (*alr2*Δ), in standard SDC (Fig. 3). SDC is polyamine-free and was chosen to maximally display the growth defect resulting from deletion of *SPE1* or *SPE2*. In addition, the Mg^{2+} concentration of SDC (4 mM) is lower than that required for optimum growth of *alr1*Δ strains (15, 16) while still allowing measurable growth. Thus, SDC should reveal any growth defects resulting from novel synthetic interactions. As previously observed for the Y534, Y535, and Y536 series of strains (Fig. 1), loss of *SPE1* in each case caused a more pronounced growth defect than loss of *SPE2* (Fig. 3, *A* and *C*). Each *spe1*Δ mutant lacked all polyamines, and each *spe2*Δ mutant contained only putrescine at a highly elevated level, confirming the knockout of *SPE1* or *SPE2*, respectively (Fig. 3, *D–F*).

Of the three double mutant strains, AH3 (*alr1*Δ *spe2*Δ), AH4 (*alr2*Δ *spe1*Δ), and AH5 (*alr2*Δ *spe2*Δ), only AH3, lacking both Alr1 and Spe2, displayed an obvious synthetic phenotype; its growth was much reduced from that of *alr1*Δ (CM200) (Fig. 3*B*) or *spe2*Δ (AH2) (Fig. 3*A*) single mutant. After 72 h of culture (starting at 0.0003 OD_{600}), the AH3 (*alr1*Δ *spe2*Δ) reached ~0.115 OD_{600} in 72 h, whereas the *alr1*Δ (CM200) and *spe2*Δ (AH2) single mutants reached ~16.6 and ~38.9 OD_{600}, respectively. To confirm that the synthetic growth defect of AH3 was caused by deletion of *SPE2* and not by other genetic alterations, we reintroduced the *SPE2* gene using a centromeric plasmid, pFL38/*SPE2*. The complemented strain (*alr1*Δ *spe2*Δ + pFL38/*SPE2*) grew at nearly the same rate as CM200 (Fig. 3*B*, *tan line*).

The synthetic growth defect of AH3 (*alr1*Δ *spe2*Δ) was associated with the loss of the ability to accumulate Mg^{2+} upon polyamine depletion. There was little or no increase in the Mg^{2+} content of AH3 (*alr1*Δ *spe2*Δ) over that of its parental strain CM200 (*alr1*Δ) (Fig. 3*H*), whereas all other *spe1*Δ and *spe2*Δ mutants derived from Alr1-expressing strains (AH1, AH2, AH4, and AH5) showed considerable increases in Mg^{2+} content (~2- and ~1.7-fold for *spe1*Δ and *spe2*Δ strains, respectively) (Fig. 3, *G* and *I*). Although the polyamine patterns were consistent with deletion of *SPE1* or

Table 3
List of PCR primers used for validation of spe1Δ and spe2Δ strains

Primer	Sequence	Product size
		bp
SPE1 ORF primer set		
Spe1F3	GTATTATCGATGAACATCTCGCCG	737
Spe1R3	AGGACCGCAGTAGTGGATTCA	
SPE2 ORF primer set		
Spe2F3	GACAAGAGCAACCACTGGAAC	565
Spe2R3	GCAGTGACTCGTTGATGCTTAGT	
Primer set to check *SPE1* deletion		
Spe1.5UTR.F3	CTCCTGCGCAATAGATTGGTC	1,854
KMX4D	CGGTGTCGGTCTCGTAG	
Primer set to check *SPE2* deletion		
Spe2.5UTR.F1	CCAAACACGGTTCTCCGGTA	1,811
KMX4D	CGGTGTCGGTCTCGTAG	
Primer set for the *spe1Δ::KanMX4* cassette		
Spe1.5UTR.F2	CATTTCTCTCCTTGTCTGTGCT	2,510
Spe1.3UTR.R4	TGGCCTGTGTTGAAGTATGGT	
Primer set for the *spe2Δ::KanMX4* cassette		
Spe2.5UTR.F3	CCAGAGATATGTAGCCTTCCATC	2,429
Spe2.3UTR.R3	GGGCATAAACCTTTGAGCATCATC	

SPE2 in each of these strains, putrescine was much higher in AH3 (Fig. 3*E*) than in other *spe2*Δ mutants. The inability of AH3 (*alr1*Δ *spe2*Δ) to enhance Mg^{2+} levels might have caused a compensatory overaccumulation of putrescine. Expression of *SPE2* in AH3 using pFL38/*SPE2* restored polyamine content (Fig. 3*E*, *tan bars*) and cell growth (Fig. 3*B*, *tan line*) and complemented the Mg^{2+} accumulation defect, indicating that these phenotypes were a specific consequence of the *spe2*Δ mutation.

In contrast to Alr1, lack of Alr2 did not impair the growth of the *spe1*Δ or *spe2*Δ mutants (Fig. 3*C*). Similar growth between AH5 (*alr2*Δ *spe2*Δ) and AH2 (*spe2*Δ) (Fig. 3, *A* and *C*) was observed, and the growth of AH4 (*alr2*Δ *spe1*Δ) appeared to be even higher than that of AH1 (*spe1*Δ). These data indicates that, unlike Alr1, Alr2 is not required for growth of polyamine-deficient cells. The significant elevation of the Mg^{2+} content in the polyamine-deficient AH4 (*alr2*Δ *spe1*Δ) and AH5 (*alr2*Δ *spe2*Δ) (Fig. 3*I*) is in accordance with the minor contribution of Alr2 to Mg^{2+} homeostasis (20, 21).

We also examined the effects of deletion of *SPE1* or *SPE2* in an *mnr2*Δ background (Fig. 4). As Mnr2 is required for the release of vacuolar Mg^{2+} stores under Mg^{2+}-deficient conditions (15), we suspected that this transporter might release Mg^{2+} from storage vacuoles to increase cytosolic Mg^{2+} concentration in response to polyamine deficiency and enhance growth of *spe1*Δ or *spe2*Δ mutants. However, no notable differences in the growth (Fig. 4, *A–B*) and the polyamine patterns (Fig. 4, *C–D*) were observed between the polyamine synthesis-deficient mutants derived from WT(NP174) and the *mnr2*Δ mutant (NP180). The growth and the polyamine patterns of AH8 (*mnr2*Δ *spe1*Δ) and AH9 (*mnr2*Δ *spe2*Δ) were similar to those of AH6 (*spe1*Δ) and AH7 (*spe2*Δ), respectively (Fig. 4, *A* and *B*), an indication that Mnr2 is not required for tolerance to polyamine deficiency. Interestingly, the *mnr2* mutation did substantially increase total cellular Mg^{2+} content over the levels observed in *spe1*Δ or *spe2*Δ single mutants (Fig. 4, *E* and *F*, compare AH8 with AH6 and AH9 with AH7). Although direct measurement of the vacuolar Mg^{2+} content has not been made, this increase is probably due to elevated uptake of Mg^{2+} by Alr1 in the *spe1*Δ or *spe2*Δ mutants and the increased sequestration of Mg^{2+} in the vacuoles of polyamine-depleted *mnr2*Δ cells (AH8 and AH9) (15). The observation that loss of Mnr2 function did not inhibit growth of polyamine-deficient strains argues that this store is not normally utilized to compensate for polyamine deficiency. Taken together, these results indicate that Alr1, but not Alr2 or Mnr2, is required for the elevated accumulation of Mg^{2+} in polyamine-deficient cells and that this response is essential for survival.

Effects of Mg^{2+} supply on polyamine metabolism

Because the above data revealed an inverse relationship between polyamine and Mg^{2+} content in polyamine-depleted *S. cerevisiae* cells, we wondered whether Mg^{2+} deficiency would lead to an increased polyamine accumulation. To address this question, we compared growth and Mg^{2+} and polyamine content of DY1457 (WT) and CM200 (*alr1*Δ) strains cultured in YPD supplemented with different concentrations of Mg^{2+} (0–200 mM). Mg^{2+} supplementation was necessary for normal growth of the *alr1*Δ mutant, as the Mg^{2+} concentration of YPD is quite low (~500 μM) (26). The growth of DY1457 was not enhanced by Mg^{2+} supplementation and was slightly inhibited with increasing concentration of Mg^{2+} (>30 mM) (Fig. 5*A*). The exogenously supplied Mg^{2+} had little influence on cellular Mg^{2+} content of WT cells (Fig. 5*B*, *brown bars*). In contrast, the growth of the *alr1*Δ mutant was severely inhibited in YPD but increased with supplemented Mg^{2+} and was restored to the WT level at 200 mM Mg^{2+} (Fig. 5*A*, *red line*). The Mg^{2+} content of the *alr1*Δ mutant cultured in standard YPD was ~1.43 mg/g dry weight (46% of WT) (Fig. 5*B*). Mg^{2+} supplementation increased the Mg^{2+} content of CM200 (*alr1*Δ) to 2.1 mg/g dry weight at 200 mM Mg^{2+} (Fig. 5*B*, *red bars*) but did not restore it to WT levels. Inability of the *alr1*Δ to fully restore the Mg^{2+} content is probably due to inefficient Mg^{2+} uptake preventing the refill of all the intracellular stores, which represent up to 80% of the total Mg^{2+} content (15). However, our results indicate that the minimal Mg^{2+} requirement for normal growth was met in the *alr1*Δ cells at this level by supplementation with 200 mM Mg^{2+}.

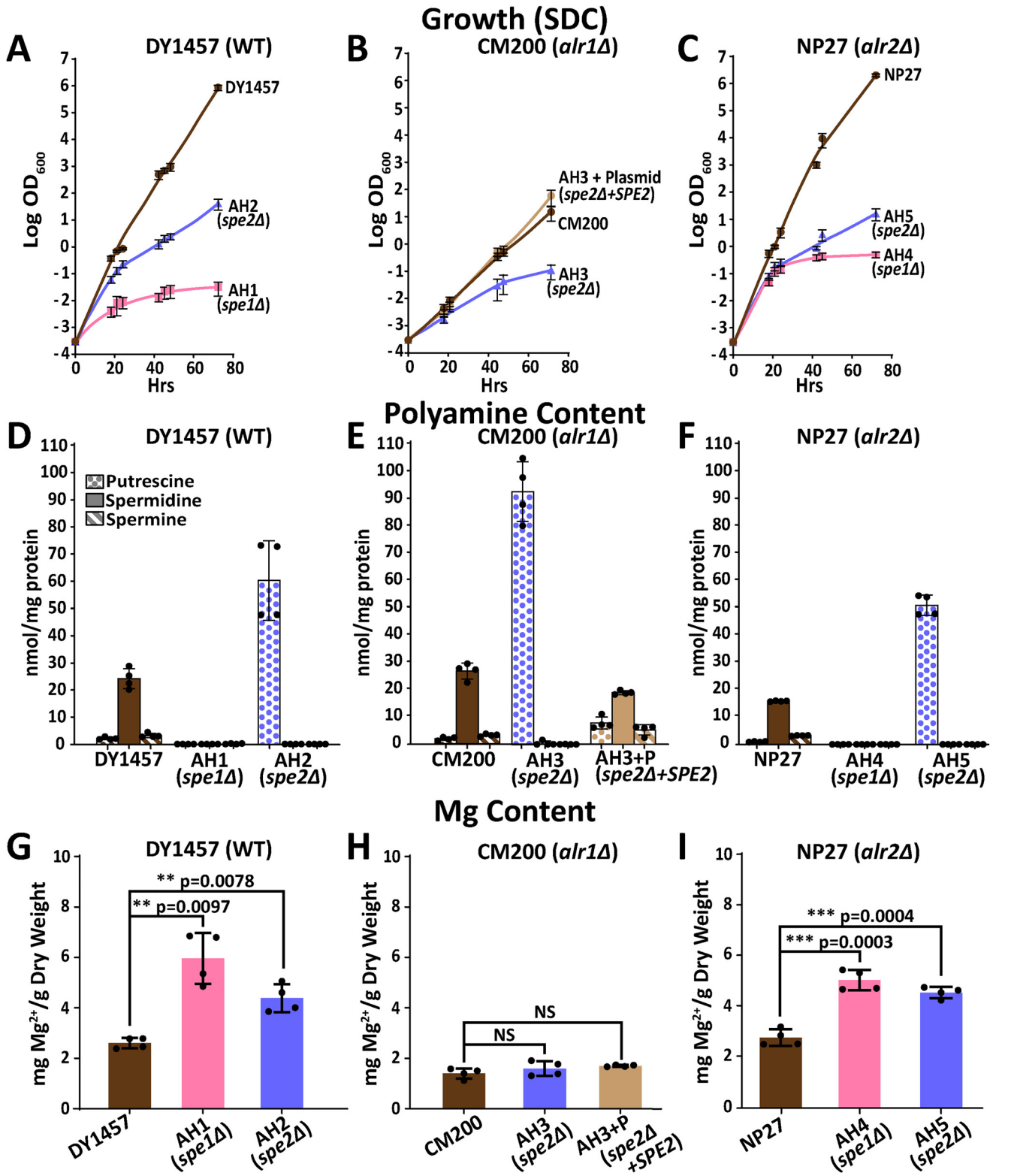

Figure 3. Effect of combined deletion of either *ALR1* or *ALR2* and either *SPE1* or *SPE2* on growth and polyamine and Mg^{2+} content. *A–C*, growth of nine strains cultured in SDC at 30 °C was measured over 72 h as in Fig. 1. Data *points* indicate means and *error bars* represent S.E. ($n = 4$). *D–F* and *G–I*, the contents of polyamines and Mg^{2+} were measured as in Fig. 1. The values of polyamine and Mg^{2+} contents are indicated as *black dots*, and each *bar* indicates the mean and the *error bars* represent S.D. ($n = 4$). The *p* values were calculated by ANOVA. *p* values less than 0.05 were considered statistically significant: **, $p \leq 0.01$; ***, $p \leq 0.001$ compared with the control. *NS* indicates that the difference is not significant.

Strikingly, the total polyamine content of Mg^{2+}-deficient CM200 (*alr1*Δ) cells cultured in standard YPD was ~67% higher than that of WT DY1457 cells (Fig. 5*C*). This heightened level decreased as the Mg^{2+} concentration in the medium increased and returned to the WT level at 100 mM Mg^{2+}, a level that almost completely suppressed the *alr1*Δ growth defect

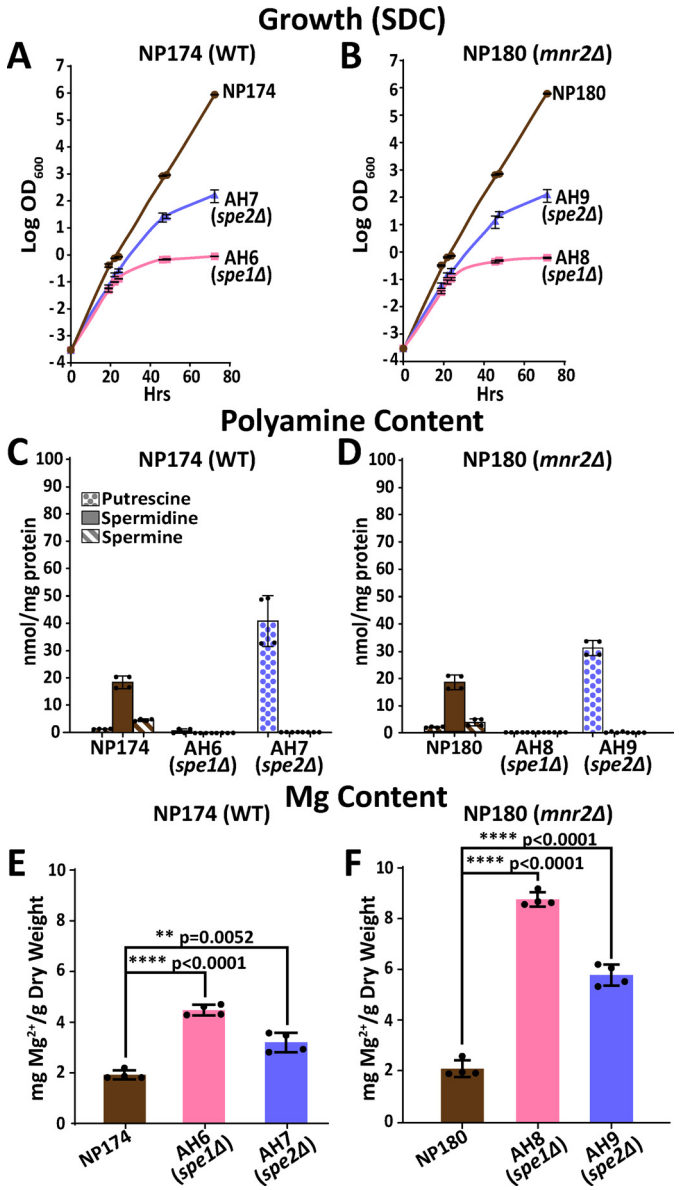

Figure 4. Effect of combined deletion of *MNR2* and either *SPE1* or *SPE2* on growth and polyamine and Mg^{2+} content. *A* and *B*, growth of six strains cultured in SDC at 30 °C was measured over 72 h as in Fig. 1. Data *points* indicate means and *error bars* represent S.E. ($n = 4$). *C–F*, the values of polyamine and Mg^{2+} contents are indicated as *black dots*, and each *bar* indicates the mean and the *error bars* represent S.D. ($n = 4$). The *p* values were calculated by ANOVA. *p* values less than 0.05 were considered statistically significant: **, $p \leq 0.01$; ****, $p \leq 0.0001$ compared with the control.

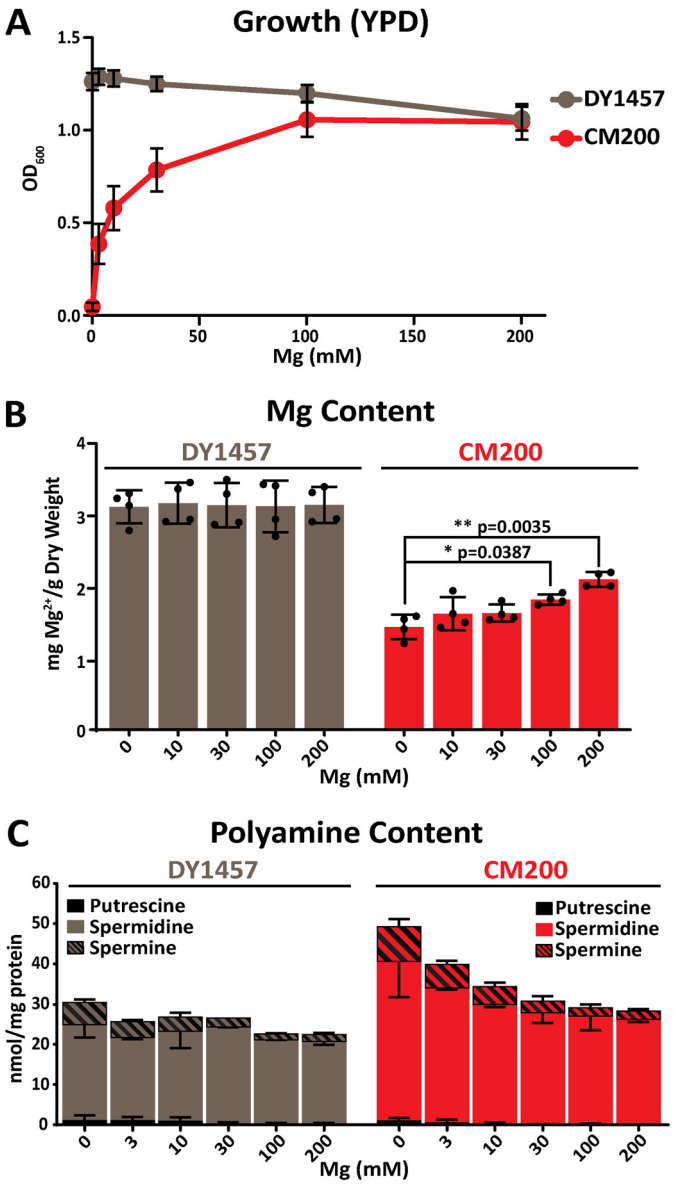

Figure 5. Effect of the *alr1*Δ mutation on growth, Mg^{2+} content, and polyamine content. *A*, growth of WT (DY1457) and *alr1*Δ (CM200) cells was measured after 18-h culture at 30 °C (initial inoculation at 0.001 OD_{600}) in YPD containing 0, 3,10, 30, 100, or 200 mM Mg^{2+}. Data *points* indicate means and *error bars* represent S.E. ($n = 4$). *B* and *C*, approximately 10 OD_{600} units of cells were harvested (at OD_{600} of ~1 or less) for analysis of Mg^{2+} content (*B*) and polyamine content (*C*) as described in Fig. 1. *B*, the values for the Mg^{2+} content are indicated as *black dots*, and each *bar* indicates the mean and the *error bars* represent S.D. ($n = 4$). *C*, the values for the total cellular polyamine content are indicated by a *merged bar* of three segments representing spermine, spermidine, and putrescine (*top* to *bottom*). Each segment represents the mean ± S.D. ($n = 4$). The *p* values were calculated for the Mg^{2+} content by ANOVA. *p* values less than 0.05 were considered statistically significant: *, $p \leq 0.05$; **, $p \leq 0.01$ compared with the control.

(Fig. 5*A*). Thus, yeast responded to Mg^{2+} deficiency by increasing polyamine content. The elevation in polyamine content in the Mg^{2+}-deficient *alr1*Δ cells suggests an interrelationship between Mg^{2+} and polyamine metabolism. A slight decrease in total polyamines was also detected in DY1457 with increasing Mg^{2+} supplementation. There was also a differential decline in the relative levels of spermine in both DY1457 and CM200 as the Mg^{2+} level in the medium increased, suggesting effects of Mg^{2+} on cellular polyamine metabolism.

Discussion

In this study, we present strong evidence that yeast cells accumulate excess Mg^{2+} to maintain viability upon depletion of cellular polyamines (Scheme 1*A*). This increase in the cellular Mg^{2+} content of polyamine-deficient *spe1*Δ and *spe2*Δ cells was reversed by the addition of spermidine in the medium (Fig. 1), suggesting a direct response to polyamine availability. Given that the cellular Mg^{2+} content is normally maintained within a narrow range in yeast (15), even in medium containing high Mg^{2+} (100–200 mM), the observed increases in cellular Mg^{2+} content (1.6–2.5-fold) in polyamine-deficient cells represent a marked deviation with likely functional significance.

The vital importance of elevated Mg^{2+} accumulation for polyamine-deficient yeast cells was indicated by the severe synthetic growth defect of an *alr1*Δ *spe2*Δ mutant, which was not able to elevate cellular Mg^{2+} content (Fig. 3) in response to polyamine deficiency. Our data further demonstrate that the polyamine depletion–induced Mg^{2+} accumulation is mainly dependent on the plasma membrane Mg^{2+} transporter Alr1 and not on its isoform Alr2 or the vacuolar Mg^{2+} transporter Mnr2. This study presents firm *in vivo* evidence for the functional interaction between Mg^{2+} and polyamines in the regulation of *S. cerevisiae* growth.

The elevation of cellular Mg^{2+} in polyamine-deficient cells is not due to a general increase in cation uptake, as other cations such as K^+ or Mn^{2+} did not increase in response to polyamine depletion. Although the Zn^{2+} content was also increased in response to polyamine depletion (Table 2), the increased Zn^{2+} content was far too low to compensate for the cation loss from polyamine depletion. The elevated Mg^{2+} would be sufficient to maintain the charge balance of polyamine-deficient cells. Furthermore, there are no reports suggesting that Zn^{2+} can substitute for polyamines in macromolecular synthesis. These findings corroborate the specificity of the Mg^{2+} function in supporting the growth of polyamine-depleted *S. cerevisiae* cells.

The specificity of Alr1 toward other divalent cations is not well-understood. Direct measurement of competitive inhibition of Mg^{2+} transport by other metals has not been conducted in yeast as no radioactive Mg^{2+} isotope is commercially available. The increased sensitivity of an Alr1-overexpressing strain toward other metals (La^{3+}, Co^{2+}, Mn^{2+}, Ni^{2+}, and Zn^{2+}) suggested a possibility of transport of these other metals by Alr1 (20). However, our metal content analysis data (Table 2) imply that Mg^{2+} and Zn^{2+}, but not Mn^{2+}, are transported by Alr1. Further studies are needed using the Alr1-overexpressing strain as well-as the *alr1*Δ strain to clarify the substrate specificity of Alr1.

In addition to the apparent regulatory effect of cellular polyamines on Mg^{2+}, an inverse relationship between polyamines and Mg^{2+} was also observed in the Mg^{2+} transport–deficient *alr1*Δ cells cultured in YPD (Fig. 5). In these cells, the total polyamine content increased in response to Mg^{2+} deficiency. These findings suggest that the polyamine pathway enzymes and/or polyamine transporters are regulated by cellular or exogenous Mg^{2+} concentration. Future investigations to identify and elucidate the specific polyamine pathways regulated by the Mg^{2+} level are warranted.

Despite the vital importance of Mg^{2+} in cellular physiology, the mechanism of Mg^{2+} homeostasis in eukaryotic cells, not to mention its functional interactions with polyamine homeostasis, is poorly understood. Although the yeast CorA family Mg^{2+} transporters have diverged considerably from the bacterial transporter CorA, they share common structural features, including two transmembrane domains connected by a short loop near the C terminus and a signature motif, GMN, that is important for Mg^{2+} selectivity (Scheme 1*B*). A cryo-EM structure of the *Thermotoga maritima* CorA suggested a mode of its regulation by intracellular Mg^{2+} concentration (27); at high Mg^{2+} concentration, Mg^{2+} is bound to cytoplasmic N-terminal domains of the CorA homopentamer, and this binding induces a closed conformation, whereas loss of Mg^{2+} binding in a low-Mg^{2+} environment reverses it to an open channel. The acidic residues involved in binding cytosolic Mg^{2+}, located at the subunit interfaces of the pentamer, were identified (28). Chemical cross-linking and the split-ubiquitin assay data (22) suggest that Alr1 and Alr2 also form homo- or heterooligomers and that, like CorA, they function as pentamers. Residues that participate in Mg^{2+} binding at the regulatory sites are conserved in prokaryotic CorA proteins (28) and in Alr1 (29), suggesting conservation of this mechanism. The CorA and Alr1/Alr2 proteins are functionally interchangeable, as overexpression of CorA partially restored the growth of an *alr1*Δ strain (16).

Our observation that polyamine deficiency increases Mg^{2+} accumulation via Alr1 suggests that this protein may be regulated directly or indirectly by cytosolic polyamine concentration. At least three possible models might explain this effect. First, polyamines might bind directly to Alr1 and inhibit its activity in a manner similar to cytosolic Mg^{2+} (27). Polyamines might interact directly with the Mg^{2+}-binding sites to mimic the effect of Mg^{2+}, or they may bind to other sites within the Alr1 cytoplasmic domains. Second, polyamines might bind directly to the Mg^{2+} channel pore itself to block it, as has been observed for some potassium channels (28). A third mechanism for increased Mg^{2+} accumulation might be the induction of expression of Alr1 mRNA and/or protein by a polyamine-dependent regulatory mechanism. Comparison of Alr1 mRNA levels in polyamine-replete and polyamine-deficient *S. cerevisiae* cells by quantitative RT-PCR did not reveal up-regulation of Alr1 expression upon depletion of polyamines (data not shown). This mechanism is also less likely than the others, considering that Alr1 transport activity was enhanced under Mg^{2+} deficient conditions, but the induction of the Alr1 protein or its mRNA was not observed (29).

A functional interaction between polyamines and Mg^{2+} has been suggested by several previous studies. In a reticulocyte lysate freed of polyamines by gel filtration, polyamines enhanced translation at suboptimal concentrations of Mg^{2+} and beyond the level achieved by high Mg^{2+} alone, suggesting that polyamines can at least partly substitute for Mg^{2+} (4, 14). Evidence for their functional interaction *in vivo* was also reported in *S. cerevisiae* (30) and mammalian cells (31) in which polyamine overloading caused cellular toxicities by displacement of cellular Mg^{2+}. The growth inhibition was attributed to excessive accumulation of polyamines leading to a concomitant decrease in cellular Mg^{2+}. It was suggested that replacement of ribosome-bound Mg^{2+} by accumulated polyamines inactivated ribosomes, leading to inhibition of protein synthesis and cell growth, but no underlying molecular mechanism was identified. Our study reveals an essential functional requirement for Mg^{2+} content elevation in polyamine-deficient cells, a biological situation opposite to that of cellular toxicity caused by excess polyamines (30). Although the two studies complement each other in supporting the concept of functional interplay between polyamines and Mg^{2+}, our study uniquely reveals a mechanism of up-regulation of cellular Mg^{2+} content involving Alr1 upon depletion of polyamines and offers an explanation for the extremely low polyamine requirement for *S. cerevisiae*

growth. In addition, this study provides new evidence that polyamine pathways are regulated by Mg^{2+} supply (Fig. 5).

The observations that *spe1*Δ and *spe2*Δ strains can survive and grow with very low amounts of cellular polyamines and that cellular Mg^{2+} accumulation is up-regulated in polyamine-deficient cells support the notion that much of the polycationic polyamine requirement of yeast can be fulfilled by Mg^{2+}. In SDC free of polyamines, the growth of *spe1*Δ and *spe2*Δ strains was arrested upon prolonged incubation in SDC despite increased Mg^{2+} content (Figs. 1, 3, and 4). Obviously, Mg^{2+} cannot totally substitute for polyamines for polyamine-specific functions, including the fine-tuning of translation (5) and the eIF5A hypusine modification. Thus, growth of *spe1*Δ and *spe2*Δ strains in SDC arrests when cellular polyamines and hypusinated eIF5A fall below the minimum threshold levels. Accumulation of reactive oxygen species and various morphological changes, including large cell size, large vacuoles, and apoptotic cell death, were reported in a *S. cerevisiae spe2*Δ strain under conditions of an extreme depletion of polyamines (32, 33). However, we found no/little changes in cell sizes and viability of the *spe1*Δ and *spe2*Δ mutants after 24-h culture in SDC, when cells were harvested for the analysis of Mg^{2+} and polyamines. This suggests that elevation of Mg^{2+} in our mutants was not associated with the loss of viability and other cellular changes that accompany extreme polyamine depletion. Instead, the elevated Mg^{2+} sustains the growth and viability of the *spe1*Δ and *spe2*Δ mutants in medium containing very low spermidine (10^{-8} M).

The fact that mammalian cells, unlike yeast, require a high level of polyamines for growth suggests either that there are mammalian-specific processes intrinsically dependent on a high polyamine concentration or that mammalian cells lack a mechanism for Mg^{2+} accumulation in response to polyamine depletion. Mg^{2+} homeostasis is poorly understood in mammalian cells, although a number of putative Mg^{2+} transporters have been described (34). In addition to the human mitochondrial CorA protein Mrs2, these include novel families unrelated to CorA, such as SLC41, TRPM6/7, MagT, NIPA, MMgT, and HIP14 families. From a screening of a Jurkat cell library, MagT1 and its homolog TUSC3 were identified as cell-surface Mg^{2+} transporters that complement the *arl1*Δ mutation (35). As their structures are unrelated to the CorA superfamily, they are not likely to respond to polyamine depletion in a similar manner as does Alr1. Although intricate mechanisms of polyamine homeostasis have been established in mammalian cells, there is poor understanding as to how polyamine pathways interact with other cellular pathways such as metal metabolism and homeostasis. Parenthetically, cellular iron levels were reported to regulate many polyamine pathway proteins in several mammalian cells (36). Future investigations will be directed toward further exploration of the interplay between Mg^{2+} and polyamine homeostasis in *S. cerevisiae* and in mammalian cells.

Experimental procedures

Yeast strains and cell growth assay

The *S. cerevisiae* strain WT Y534 (BY4741) and the two knockout strains Y535 (*spe1*Δ) and Y536 (*spe2*Δ) generated by a *S. cerevisiae* gene deletion project (25) were kindly provided by Dr. Herbert Tabor (NIDDK, National Institutes of Health). Other strains with a deletion of Mg^{2+} transport–related genes (*alr1*Δ, *alr2*Δ, and *mnr2*Δ) and new strains generated in this study are listed in Table 1. Cells were routinely cultured in YPD or SDC with or without Mg^{2+}, G418, or spermidine as indicated in specific experiments. YPD is rich in polyamines (putrescine, spermidine, and spermine, ~0.3, 2.2, and 0.4 mM, respectively) and low in Mg^{2+} (26). Standard SDC contains 4 mM Mg^{2+} but no polyamines. For the selection of Ura^+ transformants, uracil-dropout medium (SD−Ura) was used. Because the polyamine requirement for optimal growth of *spe1*Δ and *spe2*Δ strains is extremely low, ultrapure water was used, and special care was taken to avoid any environmental contamination of polyamines in SDC. To compare the growth of different strains in SDC, each strain was patched on YPD plates, and freshly grown patches of cells were inoculated in SDC at 0.001 or 0.0003 OD_{600} and cultured at 30 °C with shaking. Cell density was measured using a spectrophotometer at 600 nm every 2 h during the day. To follow growth over a 72-h period, cells were repeatedly diluted in the same fresh medium to OD_{600} 0.001 or 0.003 when the density reached ~1 OD_{600}.

Generation of spe1Δ and spe2Δ strains

The *SPE1* and *SPE2* knockout cassettes were prepared using genomic DNA of Y535 (*spe1*Δ) and Y536 (*spe2*Δ), respectively, as templates. The primers used for amplifying the *spe1*Δ*::KanMX4* cassette were CATTTCTCTCCTTGTCTGTGCT and TGGCCTGTGTTGAAGTATGGT. The primer sets for amplifying the *spe2*Δ*::KanMX4* cassette were CCAGAGATATGTAGCCTTCCATC and GGGCATAAACCTTTGAGCATCATC. PCR was performed using the Easy-A 2× Master Mix (Agilent) with the following program: 94 °C for 5 min, denaturation at 94 °C for 0.5 min, annealing at 58 °C for 1 min, an extension reaction at 72 °C for 2.5 min for 30 cycles, and a final extension reaction at 72 °C for 5 min. Yeast transformation with the purified PCR products (~2.51 and ~2.429 kb, respectively for *spe1*Δ*::KanMX4* and *spe2*Δ*::KanMX4*) was carried out with the Yeast Transformation kit (Sigma-Aldrich), according to the manufacturer's instructions, using 1 μg of linear DNA. The transformed clones were isolated on YPD plates containing 500 μg/ml G418.

Isolation of genomic DNA and PCR confirmation of genotypes of parental and spe1Δ and spe2Δ mutant strains

Cells were cultured in YPD to 1 OD at 600 nm and harvested. Genomic DNA was isolated from the cell pellets following a published protocol (37). Briefly, the cell pellets (10 OD_{600} units) were resuspended in 0.2 ml of 200 mM LiOAc, 1% SDS solution and heated at 70 °C for 5 min. 600 μl of 100% EtOH was added, and DNA and cell debris were spun down at 15,000 × *g* for 3 min. The pellets were washed with 70% EtOH. After removal of all EtOH, DNA was extracted by resuspension in 0.1 ml of Tris-EDTA buffer, and the DNA concentration was measured using a NanoDrop ND-100 spectrophotometer. PCR was performed as described above using 0.1 μg of genomic DNA, a knockout primer set or an open reading primer set (Table 3), and Jump-

Start REDTaq ReadyMix Reaction Mix (Sigma-Aldrich) according to the manufacturer's instructions.

Construction of pFL38/SPE1 and pFL38/SPE2 plasmids

To check the reversal of the phenotypes of the *spe1*Δ and *spe2*Δ strains, pFL38 plasmids encoding *SPE1* and *SPE2* were reintroduced into the corresponding null strains. The recombinant plasmids were constructed by GenScript USA Inc. by synthesis of *SPE1* and *SPE2* genes (each ORF with 200 bp 5′-UTR and 3′-UTR) and subcloning into pFL38, and the transformants were selected on SD−Ura plates.

Analysis of cellular Mg^{2+} content by inductively coupled plasma optical emission spectrometry (ICP-OES)

WT and most mutant cells were inoculated at a density of 0.001 in 10–20 ml of the indicated medium, and exponentially growing cells (1 or less than 1 OD_{600}) were harvested at ~24 h after inoculation. For slow-growing mutant strains, a higher inoculum density and a larger culture volume were used to obtain ~10–20 OD_{600} units of cells in 24 h. Cells were harvested by centrifugation, transferred to preweighed Eppendorf tubes, and washed once with 1 mM EDTA and twice with ultrapure water, and the washed cell pellets were frozen on dry ice. The total Mg^{2+} content was measured by ICP-OES as described previously (38).

Determination of yeast polyamine content

S. cerevisiae cells were cultured, harvested, and frozen, in parallel or similarly to those for Mg^{2+} analysis, as described above. Polyamines were extracted from the cell pellets by resuspension in 1.2 N perchloric acid, repeated vortexing with glass beads, and incubation on ice. The extracted amines and the internal standard (1,7-diaminoheptane) were derivatized using dansyl chloride, and the dansylated polyamine derivatives were analyzed in duplicate by reverse-phase HPLC as described previously (39). The polyamine content was normalized against cell proteins determined using the Pierce BCA protein assay dye reagent after dissolving the perchloric acid precipitates in 0.1 N NaOH.

Statistical analysis

All values are presented as means of four or more biological replicates (n) as indicated in the legends. The contents of Mg^{2+} and polyamines are expressed as mean ± S.D., and the optical densities of cells are expressed as mean ± S.E. Differences between samples were compared using analysis of variance (ANOVA) and were considered statistically significant at $p < 0.05$. All statistical analyses were conducted using GraphPad Prism 8 (GraphPad Software, San Diego, CA).

Author contributions—A. S. H., R. A. C., C. W. M., and M. H. P. conceptualization; A. S. H., M. D., C. W. M., and M. H. P. data curation; A. S. H., M. D., and M. H. P. formal analysis; A. S. H. and M. H. P. validation; A. S. H., R. A. C., and M. H. P. investigation; A. S. H. visualization; A. S. H., M. D., R. A. C., C. W. M., and M. H. P. methodology; A. S. H., R. A. C., C. W. M., and M. H. P. writing-review and editing; R. A. C. and M. H. P. supervision; R. A. C., C. W. M., and M. H. P. funding acquisition; C. W. M. resources; M. H. P. writing-original draft; M. H. P. project administration.

Acknowledgments—We thank Dr. Edith C. Wolff (NIDCR, National Institutes of Health) for helpful suggestions on the manuscript, Drs. Kazuei Igarashi (Chiba University) and Anthony E. Pegg (Pennsylvania State University) for suggestions on the potential role of Mg^{2+} and Mg^{2+} transporter in polyamine-deficient yeast cells, Dr. David Killilea at CHORI (Children's Hospital Oakland Research Institute) Elemental Analysis Facility for analysis of Mg^{2+} and other elements, and Dr. Dong-Yun Kim (NHLBI, National Institutes of Health) for helpful advice on statistical analyses.

References

1. Casero, R. A., Jr., Murray Stewart, T., and Pegg, A. E. (2018) Polyamine metabolism and cancer: treatments, challenges and opportunities. *Nat. Rev. Cancer* **18,** 681–695 CrossRef Medline
2. Pegg, A. E., and Casero, R. A., Jr. (2011) Current status of the polyamine research field. *Methods Mol. Biol.* **720,** 3–35 CrossRef Medline
3. Tabor, C. W., and Tabor, H. (1984) Polyamines. *Annu. Rev. Biochem.***53,** 749–790 CrossRef Medline
4. Igarashi, K., and Kashiwagi, K. (2015) Modulation of protein synthesis by polyamines. *IUBMB Life* **67,** 160–169 CrossRef Medline
5. Dever, T. E., and Ivanov, I. P. (2018) Roles of polyamines in translation. *J. Biol. Chem.* **293,** 18719–18729 CrossRef Medline
6. Kahana, C. (2009) Regulation of cellular polyamine levels and cellular proliferation by antizyme and antizyme inhibitor. *Essays Biochem.* **46,** 47–61 CrossRef Medline
7. Mandal, S., Mandal, A., Johansson, H. E., Orjalo, A. V., and Park, M. H. (2013) Depletion of cellular polyamines, spermidine and spermine, causes a total arrest in translation and growth in mammalian cells. *Proc. Natl. Acad. Sci. U.S.A.* **110,** 2169–2174 CrossRef Medline
8. Chattopadhyay, M. K., Park, M. H., and Tabor, H. (2008) Hypusine modification for growth is the major function of spermidine in *Saccharomyces cerevisiae* polyamine auxotrophs grown in limiting spermidine. *Proc. Natl. Acad. Sci. U.S.A.* **105,** 6554–6559 CrossRef Medline
9. Park, M. H., Cooper, H. L., and Folk, J. E. (1981) Identification of hypusine, an unusual amino acid, in a protein from human lymphocytes and of spermidine as its biosynthetic precursor. *Proc. Natl. Acad. Sci. U.S.A.* **78,** 2869–2873 CrossRef Medline
10. Nishimura, K., Lee, S. B., Park, J. H., and Park, M. H. (2012) Essential role of eIF5A-1 and deoxyhypusine synthase in mouse embryonic development. *Amino Acids* **42,** 703–710 CrossRef Medline
11. Park, M. H., and Wolff, E. C. (2018) Hypusine, a polyamine-derived amino acid critical for eukaryotic translation. *J. Biol. Chem.* **293,** 18710–18718 CrossRef Medline
12. Romani, A. M. (2011) Cellular magnesium homeostasis. *Arch. Biochem. Biophys.* **512,** 1–23 CrossRef Medline
13. Gardner, R. C. (2003) Genes for magnesium transport. *Curr. Opin. Plant Biol.* **6,** 263–267 CrossRef Medline
14. Igarashi, K., Hikami, K., Sugawara, K., and Hirose, S. (1973) Effect of polyamines on polypeptide synthesis in rat liver cell-free system. *Biochim. Biophys. Acta* **299,** 325–330 CrossRef Medline
15. Pisat, N. P., Pandey, A., and Macdiarmid, C. W. (2009) MNR2 regulates intracellular magnesium storage in *Saccharomyces cerevisiae*. *Genetics* **183,** 873–884 CrossRef Medline
16. Graschopf, A., Stadler, J. A., Hoellerer, M. K., Eder, S., Sieghardt, M., Kohlwein, S. D., and Schweyen, R. J. (2001) The yeast plasma membrane protein Alr1 controls Mg^{2+} homeostasis and is subject to Mg^{2+}-dependent control of its synthesis and degradation. *J. Biol. Chem.* **276,** 16216–16222 CrossRef Medline
17. Payandeh, J., Pfoh, R., and Pai, E. F. (2013) The structure and regulation of magnesium selective ion channels. *Biochim. Biophys. Acta* **1828,** 2778–2792 CrossRef Medline
18. Lee, J. M., and Gardner, R. C. (2006) Residues of the yeast ALR1 protein that are critical for magnesium uptake. *Curr. Genet.* **49,** 7–20 CrossRef Medline

19. Palombo, I., Daley, D. O., and Rapp, M. (2013) Why is the GMN motif conserved in the CorA/Mrs2/Alr1 superfamily of magnesium transport proteins? *Biochemistry* **52,** 4842–4847 CrossRef Medline
20. MacDiarmid, C. W., and Gardner, R. C. (1998) Overexpression of the *Saccharomyces cerevisiae* magnesium transport system confers resistance to aluminum ion. *J. Biol. Chem.* **273,** 1727–1732 CrossRef Medline
21. da Costa, B. M., Cornish, K., and Keasling, J. D. (2007) Manipulation of intracellular magnesium levels in Saccharomyces cerevisiae with deletion of magnesium transporters. *Appl. Microbiol. Biotechnol.* **77,** 411–425 CrossRef Medline
22. Wachek, M., Aichinger, M. C., Stadler, J. A., Schweyen, R. J., and Graschopf, A. (2006) Oligomerization of the Mg^{2+}-transport proteins Alr1p and Alr2p in yeast plasma membrane. *FEBS J.* **273,** 4236–4249 CrossRef Medline
23. Bui, D. M., Gregan, J., Jarosch, E., Ragnini, A., and Schweyen, R. J. (1999) The bacterial magnesium transporter CorA can functionally substitute for its putative homologue Mrs2p in the yeast inner mitochondrial membrane. *J. Biol. Chem.* **274,** 20438–20443 CrossRef Medline
24. Klompmaker, S. H., Kohl, K., Fasel, N., and Mayer, A. (2017) Magnesium uptake by connecting fluid-phase endocytosis to an intracellular inorganic cation filter. *Nat. Commun.* **8,** 1879 CrossRef Medline
25. Giaever, G., and Nislow, C. (2014) The yeast deletion collection: a decade of functional genomics. *Genetics* **197,** 451–465 CrossRef Medline
26. Eide, D. J., Clark, S., Nair, T. M., Gehl, M., Gribskov, M., Guerinot, M. L., and Harper, J. F. (2005) Characterization of the yeast ionome: a genome-wide analysis of nutrient mineral and trace element homeostasis in Saccharomyces cerevisiae. *Genome Biol.* **6,** R77 CrossRef Medline
27. Matthies, D., Dalmas, O., Borgnia, M. J., Dominik, P. K., Merk, A., Rao, P., Reddy, B. G., Islam, S., Bartesaghi, A., Perozo, E., and Subramaniam, S. (2016) Cryo-EM structures of the magnesium channel CorA reveal symmetry break upon gating. *Cell* **164,** 747–756 CrossRef Medline
28. Nichols, C. G., and Lee, S. J. (2018) Polyamines and potassium channels: a 25-year romance. *J. Biol. Chem.* **293,** 18779–18788 CrossRef Medline
29. Lim, P. H., Pisat, N. P., Gadhia, N., Pandey, A., Donovan, F. X., Stein, L., Salt, D. E., Eide, D. J., and MacDiarmid, C. W. (2011) Regulation of Alr1 Mg transporter activity by intracellular magnesium. *PLoS One* **6,** e20896 CrossRef Medline
30. Maruyama, T., Masuda, N., Kakinuma, Y., and Igarashi, K. (1994) Polyamine-sensitive magnesium transport in *Saccharomyces cerevisiae*. *Biochim. Biophys. Acta* **1194,** 289–295 CrossRef Medline
31. He, Y., Kashiwagi, K., Fukuchi, J., Terao, K., Shirahata, A., and Igarashi, K. (1993) Correlation between the inhibition of cell growth by accumulated polyamines and the decrease of magnesium and ATP. *Eur. J. Biochem.* **217,** 89–96 CrossRef Medline
32. Balasundaram, D., Tabor, C. W., and Tabor, H. (1993) Oxygen toxicity in a polyamine-depleted *spe2*Δ mutant of *Saccharomyces cerevisiae*. *Proc. Natl. Acad. Sci. U.S.A.* **90,** 4693–4697 CrossRef Medline
33. Chattopadhyay, M. K., Tabor, C. W., and Tabor, H. (2006) Polyamine deficiency leads to accumulation of reactive oxygen species in a *spe2*Δ mutant of *Saccharomyces cerevisiae*. *Yeast* **23,** 751–761 CrossRef Medline
34. Quamme, G. A. (2010) Molecular identification of ancient and modern mammalian magnesium transporters. *Am. J. Physiol. Cell Physiol.* **298,** C407–C429 CrossRef Medline
35. Zhou, H., and Clapham, D. E. (2009) Mammalian MagT1 and TUSC3 are required for cellular magnesium uptake and vertebrate embryonic development. *Proc. Natl. Acad. Sci. U.S.A.* **106,** 15750–15755 CrossRef Medline
36. Lane, D. J. R., Bae, D. H., Siafakas, A. R., Suryo Rahmanto, Y., Al-Akra, L., Jansson, P. J., Casero, R. A., Jr., and Richardson, D. R. (2018) Coupling of the polyamine and iron metabolism pathways in the regulation of proliferation: Mechanistic links to alterations in key polyamine biosynthetic and catabolic enzymes. *Biochim. Biophys. Acta Mol. Basis Dis.* **1864,** 2793–2813 CrossRef Medline
37. Lõoke, M., Kristjuhan, K., and Kristjuhan, A. (2011) Extraction of genomic DNA from yeasts for PCR-based applications. *BioTechniques* **50,** 325–328 CrossRef Medline
38. Wang, Y., Weisenhorn, E., MacDiarmid, C. W., Andreini, C., Bucci, M., Taggart, J., Banci, L., Russell, J., Coon, J. J., and Eide, D. J. (2018) The cellular economy of the *Saccharomyces cerevisiae* zinc proteome. *Metallomics* **10,** 1755–1776 CrossRef Medline
39. Kabra, P. M., Lee, H. K., Lubich, W. P., and Marton, L. J. (1986) Solid-phase extraction and determination of dansyl derivatives of unconjugated and acetylated polyamines by reversed-phase liquid chromatography: improved separation systems for polyamines in cerebrospinal fluid, urine and tissue. *J. Chromatogr.* **380,** 19–32 CrossRef Medline